Article

Experimental Verification of the Shielding Properties of Selected Textile Materials in the X Frequency Band

Dariusz Wójcik [1], Maciej Surma [1], Mirosław Magnuski [1], Tomasz Blachowicz [2], Khorolsuren Tuvshinbayar [3], Marius Dotter [3], Yusuf Topuz [3] and Andrea Ehrmann [3,*]

1 Department of Electronics, Electrical Engineering and Microelectronics, Faculty of Automatic Control, Electronics and Computer Science, Silesian University of Technology, 44-100 Gliwice, Poland; dariusz.wojcik@polsl.pl (D.W.); maciej.surma@polsl.pl (M.S.); miroslaw.magnuski@polsl.pl (M.M.)

2 Institute of Physics—Center for Science and Education, Silesian University of Technology, 44-100 Gliwice, Poland; tomasz.blachowicz@polsl.pl

3 Faculty of Engineering Sciences and Mathematics, Bielefeld University of Applied Sciences and Arts, 33619 Bielefeld, Germany; khorolsuren.tuvshinbayar@hsbi.de (K.T.); marius.dotter@hsbi.de (M.D.); yusuf.topuz@hsbi.de (Y.T.)

* Correspondence: andrea.ehrmann@hsbi.de

Abstract: The increasing development and application of wireless devices and systems that radiate electromagnetic waves makes electromagnetic interference (EMI) shielding more and more important in everyday life. In practice, rigid EMI shields are the most commonly used ones. However, for humans or in automotive and aviation applications, flexible, drapable materials, such as textile fabrics, can be more effective and useful. Textile fabrics are usually nonconductive and not magnetic, i.e., they lack the requirements for EMI shielding. However, shielding properties of textile fabrics can be achieved by blending yarns with fine wires or coating fibers or by blending complete textile layers with conductive or magnetic materials. In this paper, shielding textile fabrics and 3D-printed materials, as references with different conductive (and partly also magnetic) properties, are examined. The measurements show a high shielding effectiveness of 80 dB given by densely woven fabrics with a thin metallic coating in the frequency range of 6.5–11 GHz, while large pores in crocheted fabrics significantly reduce the EMI shielding effectiveness, and other samples did not show shielding at all, suggesting that a combination of conductivity and the structure of the samples is responsible for the shielding potential.

Keywords: electromagnetic interference (EMI); shielding effectiveness; conductive coating; metallized fabric; conductive yarn; crocheted fabric; porosity; cover factor

1. Introduction

In recent years, more and more emitters of electromagnetic (EM) irradiation are being found in companies and laboratories but also in everyday life environments. While the potential danger of electromagnetic irradiation for people is still under discussion, protection of electronic equipment from external EM irradiation is often important in terms of cyber security.

Electromagnetic interference (EMI) shielding reduces the exposure of volatile devices or living tissues to electromagnetic radiation. Shielding mechanisms can be subdivided into reflection, absorption, multiple reflections, or combinations thereof [1–3]. To avoid unwanted secondary electromagnetic (EM) irradiation due to reflection, absorption is often preferred among these mechanisms [4,5]. The EM disturbances that should be suppressed can be observed in all electrical and electronic devices and systems in a very broad frequency range up to 1 THz [6–11].

Although machines are often shielded by rigid materials, in many situations, lightweight, drapable, elastic materials, such as macroscopic textile fabrics or nanofibrous membranes with suitable electrical and magnetic properties, are preferable [12,13].

Usually, textile fabrics are isolating. Nevertheless, it is possible to coat them with conductive materials or to integrate conductive materials in the form of nanoparticles or fibers, thus making them conductive.

High shielding effectiveness is often approached by coating textiles with MXenes. MXenes belong to the two-dimensional materials that have been under intense investigation in recent years and contain early transition metal carbides, nitrides, and carbonitrides, showing different metallic or ceramic properties for different chemical constitutions [12]. They can oxidize in humid environments and thus have to be protected from water vapor. Nevertheless, they are found in many recent studies on EMI shielding textile fabrics. Wang et al., for example, coated polypyrrole(PPy)-modified Mxene sheets on textile fabrics from poly(ethylene terephthalate) (PET) before applying an additional silicone coating as a protection layer, thus reaching a high electrical conductivity of approximately 1000 S/m and an EMI shielding effectiveness of around 90 dB, besides good Joule heating performance [14]. By dip-coating cotton and linen fabrics in MXene dyes, Uzun et al. reached 40 db EMI shielding in the X band (8.2 GHz–12.4 GHz) for four coating cycles and 80 dB shielding after 24 coating cycles; they also reached long-term stability, with only an 8–13% reduction of these values after storing the samples under ambient conditions [15]. While EMI shielding is mostly in the focus of such studies, researchers sometimes also mention good heating performance due to the gained conductivity of the coated textile fabrics and even bactericidal efficacy, e.g., against *E. coli* and *S. aureus*, as Yu et al. showed for MXene-decorated polydopamine-modified cellulose nonwovens [16].

Besides the relatively new approaches to improving EMI shielding through MXene coating, several researchers report more conventional coatings, including metals. Such metal coatings can contain copper, for example, which is applied in a strong alkali bath and subsequently stabilized on the fibers by silanization, a process that can increase or decrease the original EMI shielding effectiveness by a factor of 2, depending on the chosen silane [17]. Electroless plating with copper particles on a polyester nonwoven was suggested by Hu et al., resulting in EMI shielding in the frequency range of 0.5–1.5 GHz at 30–55 dB [18]. Applying silver nanoparticles on an oxidized cellulose textile surface, Hong et al. reached 47–69 dB shielding for a single- or triple-layer system [19].

Coatings containing carbon, such as graphite or carbon black, are also very common in the textile industry and can be used to increase the conductivity of a textile fabric [20]. Using carbon nanotubes (CNTs), Moonlek et al. found 8–10 dB for silk fabric/natural rubber latex/CNT composites with a thickness of 2–8 mm [21]. An improved CNT distribution on a cotton woven fabric was reached by polymerizing polyaniline (PAni) on the CNTs, resulting in a 23 dB shielding effectiveness for a single-layer fabric [22].

While such coatings are often used in the textile industry, metal or carbon fibers can be included in yarns and fabrics. Carbon fiber laminates were stitched with copper, titanium, and Kevlar metallic and non-conductive threads formed to composites by vacuum-assisted infusion, resulting in EMI shielding effectiveness values of 40–47 dB in the X band [23]. Interestingly, while copper threads resulted in slightly larger shielding values, the shielding effectiveness was generally improved in the compact fiber arrangement of the stitched multi-layer composites. Combining carbon fiber waste with nylon fibers to create a needle-punched nonwoven, Pakdel et al. found EMI shielding values around 25–80 dB for different carbon fiber fractions and sample thicknesses [24]. Adding a polymer, as a binder, to recycled carbon fiber waste, Hu et al. reached 30–70 dB shielding, depending on the sample thickness and the polymeric binder [25].

Finally, intrinsically conductive polymers can be used as a coating. Applying one–five layers of PAni or PPy on a woven poly(acrylonitrile) (PAN) fabric using a special inkjet printing process, Rybicki et al. reached an EMI shielding effectiveness of 5–22 dB for PAni and 2.25–7 dB for PPy [26]. Siavashani et al. combined PPy with silver nanoparticles and poly(3,4-ethylenedioxythiophene):polystyrenesulfonic acid (PEDOT:PSS), leading to a shielding effectiveness of 40 dB [27]. A similar value was reached by Yu et al., who tested varying PPy concentrations dip-coated on a cotton fabric and the subsequent in situ

polymerization of poly(N-isopropylacrylamide) (PNIPAAm) on the PPy-coated fabric [28]. However, these coatings require relatively complicated preparation of yarns or fabrics if adequate shielding effectiveness values are to be reached [12,13].

In this paper, we report investigations of commercially available woven fabrics as well as conductive and magnetic yarns, which were processed by hand-crocheting, and commercially available conductive coatings on textile fabrics. The broad variety of different textile and 3D-printed samples allows for a better comparison of specimens with strongly differing thickness, porosity, and material composition, thus enabling quite general statements about the influence of these parameters on the EMI shielding properties of laminar objects.

The applied measurement test set was dedicated to the X frequency band. Validation was carried out by means of measurements on standard aluminum foil for food applications.

2. Theoretical Background of the Experiment

Considering a shielding material S illuminated by an electromagnetic wave (Figure 1), shielding quality can be described using the shielding effectiveness (SE) parameter

$$SE = -10\log\left(\frac{P_\mathrm{T}}{P_\mathrm{I}}\right), \tag{1}$$

where P_I is the incident power, P_T is the transmitted power, and P_R is the reflected electromagnetic power.
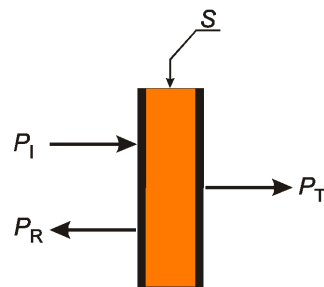

Figure 1. Schematic diagram showing the incident, reflected, and transmitted electromagnetic radiations.

According to the Schelkunoff theory [29], the SE can be expressed as

$$SE = SE_\mathrm{R} + SE_\mathrm{M} + SE_\mathrm{A} \approx SE_\mathrm{R} + SE_\mathrm{A}, \tag{2}$$

where SE_R is the reflection loss, SE_M is the multiple reflection loss, and SE_A is the absorption loss inside the material. For very conductive materials for which SE_A is large, multiple reflection losses can be avoided. For the plane wave normal incident case, the SE_A and SE_R parameters can be calculated from the following expressions [29]:

$$SE_\mathrm{A} = 8.69\, t\, \sqrt{\pi f \mu \sigma}, \tag{3}$$

$$SE_\mathrm{R} = 20\log\left|\frac{[\eta_0 + \eta_s]^2}{4\eta_0\eta_s}\right|, \tag{4}$$

$$\eta_s = \sqrt{\frac{j2\pi f \mu}{\sigma + j2\pi f \epsilon}}, \tag{5}$$

where material properties are characterized by the permeability μ, the permittivity ϵ, and the conductivity σ. Hence, η_S is the intrinsic impedance of the material, η_0 is the intrinsic impedance of free space, f is the operating frequency, and $j = \sqrt{-1}$ is the imaginary part unit.

Since direct measurements of electrical and magnetic parameters of textile materials are very difficult to perform at microwave frequencies, the shielding properties could be expressed in terms of the scattering parameters S_{ij} [2,10,30], where i represents the output and j represents the input in a two-port network. Therefore, S_{11} is the reflection coefficient at the first port, S_{12} is the reversed isolation, S_{21} is the insertion loss, and S_{22} is the reflection coefficient at the second port. The total shielding effectiveness SE' can be calculated as follows:

$$SE' = SE'_R + SE'_A = -10\log|S_{21}|^2 \tag{6}$$

$$SE_A\prime = -10\log\left(\frac{|S_{21}|^2}{1 - |S_{11}|^2}\right) \tag{7}$$

$$SE_R\prime = -10\log\left(1 - |S_{11}|^2\right) \tag{8}$$

where $SE_R\prime$ is the reflection loss and $SE_A\prime$ is the absorption loss inside the material. Applying the properties of the scattering parameters [29]

$$|S_{21}|^2 = \frac{P_T}{P_I}, \tag{9}$$

$$|S_{11}|^2 = \frac{P_R}{P_I}, \tag{10}$$

it can be easily shown that

$$SE'_R = -10\log\left(\frac{P_R}{P_{IN}}\right) = -10\log\left(\frac{P_R}{P_I - P_R}\right), \tag{11}$$

$$SE'_A = -10\log\left(\frac{P_T}{P_{IN}}\right) = -10\log\left(\frac{P_T}{P_I - P_R}\right), \tag{12}$$

where P_{IN} is the power penetrating the shielding material. It should be noted that the total shielding effectiveness is defined identically in both theories but the quantities SE_A and $SE_A\prime$ have a slightly different physical meaning in each theory. The same remark applies to SE_R and $SE_R\prime$ [31].

3. Materials and Methods

3.1. Samples under Investigation

The samples chosen for this study should reflect many different structural and material properties: nanofiber mats are very thin and have small pores in the nanometer range, while crocheted fabrics are relatively thick and have large holes in the range of several millimeters. Metalized woven fabrics have a homogeneous conductive coating, while 3D-printed conductive or magnetic materials usually show nonconductive or nonmagnetic areas next to percolation paths but have smaller pores than crocheted fabrics. Conductive coatings on nonconductive textile fabrics will lead to relatively homogeneous conductive properties of the samples, but they will have much higher resistivity than the metallized fabrics. By choosing these samples, a broad variety of different materials and structural parameters is tested.

Nanofiber mats were produced by the needleless electrospinning machine NanoSpider Lab (Elmarco, Czech Republic) from a spinning solution of 14% poly(acrylonitrile) (PAN, X-PAN, Dralon, Dormagen, Germany) in dimethyl sulfoxide (DMSO, minimum 99.9%, S3 Chemicals, Bad Oeynhausen, Germany) with additional nickel ferrite nanoparticles (Fe_2O_3/NiO, Merck KGaA, Darmstadt, Germany) in different mass ratios.

The applied coatings are PEDOT:PSS (Orgacon S305), an intrinsically conductive polymer, and Powersil 466 A/B (Wacker Chemie AG, München, Germany), a liquid silicone rubber based on poly(dimethylsiloxane).

The conductive yarns used in this study are Shieldex 235/34 dtex (Statex, Bremen, Germany), containing silver-coated polyamide 6.6 fibers, and S-Shield Nm 50/2 (Schoeller,

Bregenz, Austria), containing 80% polyester (PES) fibers and 20% steel fibers, which is also ferromagnetic.

The commercially available woven fabrics under examination are Ripstop Silver Fabric (Less EMF, NY, USA) and Pure Copper Polyester Taffeta (Less EMF).

All 3D-printed samples were produced by an Orcabot XXL Pro 2 (Prodim, the Netherlands) fused deposition modeling (FDM) printer, preparing 3 layers in $\pm45°$ orientation with an overall thickness of 0.6 mm. The polymers used for 3D-printed samples are pure poly(lactic acid) (PLA) (Grauts GmbH, Löhne, Germany), conductive PLA (Proto-pasta, Vancouver, Canada), and magnetic PLA (Proto-pasta).

The investigated samples are shown in Table 1. Microscopic images were taken with a Camcolms2 digital microscope. Sheet resistance values of the samples were measured with a 4-point MR1measurement system with special textile electrodes (Schuetz Messtechnik, Teltow, Germany).

Table 1. Samples under investigation. The long side of all images is 8 mm in length.
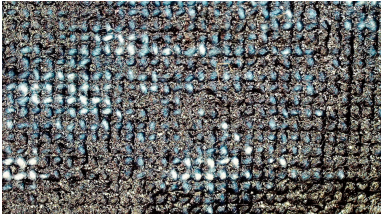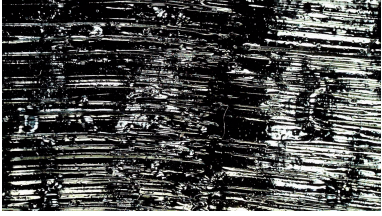
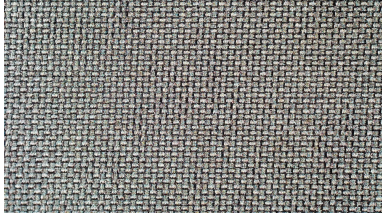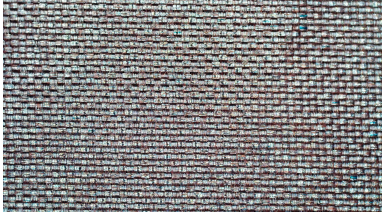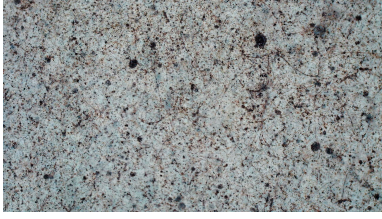| Name	Description	Micrograph
PEDOT:PSS	Cotton woven fabric with PEDOT:PSS coating (40 warp threads/cm, 40 weft threads/cm)	
Powersil	Cotton woven fabric with Powersil coating (40 warp threads/cm, 40 weft threads/cm)	
PEDOT:PSS/Powersil	Cotton woven fabric with PEDOT:PSS and subsequent Powersil coating (40 warp threads/cm, 40 weft threads/cm)	
Conductive yarn	Hand-crocheted fabric from 2 Shieldex yarns (2.6 wales/cm, 2.2 courses/cm)	
Magnetic yarn	Hand-crocheted fabric from 2 S-Shield yarns (2.6 wales/cm, 2.2 courses/cm)	

Table 1. *Cont.*
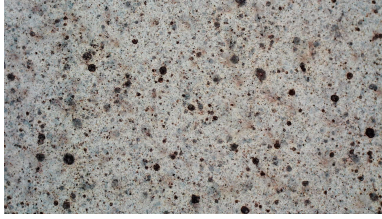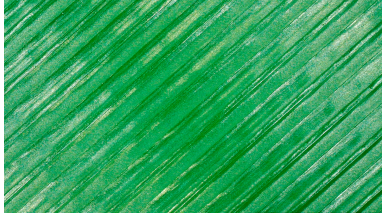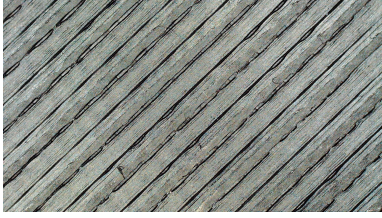
Name	Description	Micrograph
Magnetic + conductive yarn	Hand-crocheted fabric from 1 Shieldex + 1 S-Shield yarn (3.0 wales/cm, 1.8 courses/cm)	
Silver fabric	Silver-metalized woven fabric (74 warp threads/cm, 89 weft threads/cm)	
Copper fabric	Copper-metalized woven fabric (65 warp threads/cm, 78 weft threads/cm)	
PAN:nickel-ferrite 1:1	Electrospun PAN nanofiber mat with nickel ferrite, mass ratio 1:1	
PAN:nickel-ferrite 1:1.8	Electrospun PAN nanofiber mat with nickel ferrite, mass ratio 1:1.8	
PLA	3 layers, FDM-printed	
Conductive PLA	3 layers, FDM-printed	

Table 1. *Cont.*

Name	Description	Micrograph
Magnetic PLA	3 layers, FDM-printed	

It is clearly visible from these microscopic images that the hand-crocheted fabrics have large pores in the range of 1–2 mm, as compared to holes of approximately 100 μm diameter in the 3D-printed conductive PLA and of a few micrometers in the metallized woven fabrics, while nanofibrous membranes typically have pores in the range of a few tens of nanometers. Besides, the PAN:nickel ferrite nanofiber mats have agglomerations of the magnetic nanoparticles, separated by areas with significantly lower amount of magnetic material. On the other hand, the Powersil coating as well as the metalized woven fabrics have very small pores that are not visible in the picture for the presented magnification, implying better EMI shielding properties than the other materials.

3.2. EMI Shielding Measurements

The measurements of scattering parameters were performed using the waveguide variant of the transmission/reflection method [31–34] by means of the test set shown in Figure 2. The test set consists of two sections (W) of the WR-90 waveguide that are both 250 mm in length and two broadband SMA/WR-90 transitions (T). The sample under investigation is placed in a fixture (S) shown in Figure 2b and connected to ports 1 and 2 of the WR-90 waveguide. Therefore, it is placed directly between the flanges of the waveguides (W) at the symmetry plane of the test set. The applied waveguides operate in the X band range of frequencies with the fundamental mode TE_{10}.
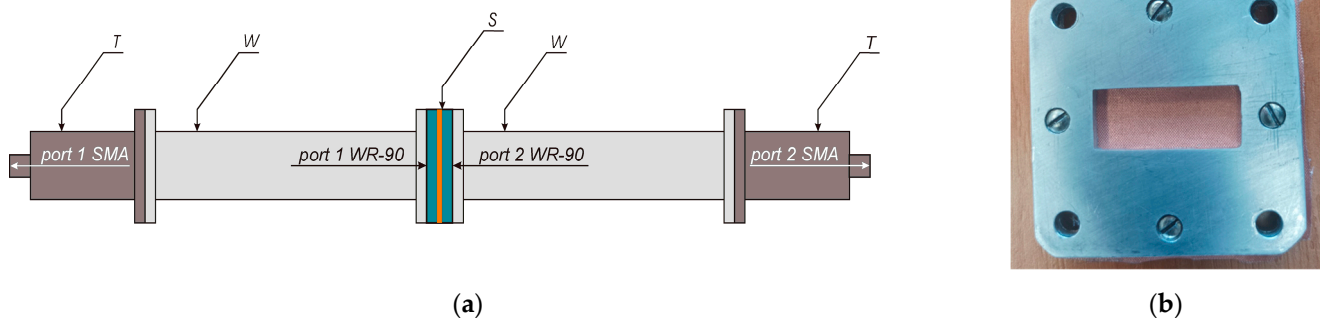

(**a**)

(**b**)

Figure 2. (**a**) Transmitting/reflecting waveguide measurement test set with the fabric sample inserted to be characterized; (**b**) fabric fixture.

The scattering parameters of interest can be determined with the vector network analyzer (VNA) directly connected to ports SMA1 and SMA2 of the test set. Since the application of the VNA without additional instrumentation for measurements of materials with high shielding effectiveness showed a strongly increased noise level, the following measures were applied: narrowing the intermediate frequencies (IF) bandwidth of the VNA, averaging the measurement results, and increasing the meter signal source power to the maximum. Additionally, two 35 dB cascaded multistage amplifiers (Amplica XM564302) operating in the frequency range from 6 to 12.4 GHz were applied. Due to the large number of stages, the amplifiers are treated as unilateral. Figure 3 shows the setup, including the amplifiers connected to the output port of the waveguide part of the test set.
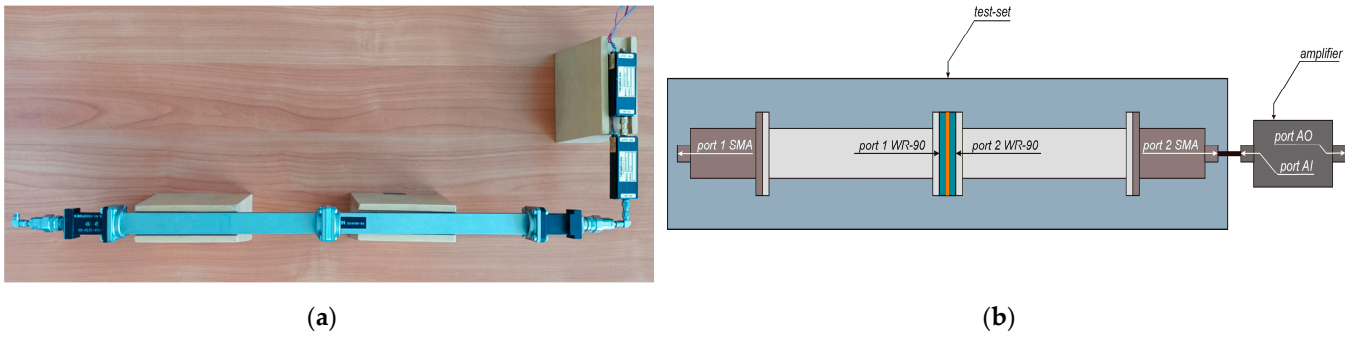
(**a**) (**b**)

Figure 3. (**a**) Test set with amplifier connected; (**b**) model of the system.

In Figure 4, the signal flow graph of the whole system is presented. Due to the unilaterality of the amplifier, $S_{21AM} = 0$ is assumed. Using the measured parameters of the S_{TA} matrix to characterize the whole system, the scattering matrix S_{TS} of the waveguide test set can be determined as

$$S_{11TS} = S_{22TS} \approx S_{11TA}, \tag{13}$$

$$S_{21TS} = S_{12TS} \approx \frac{S_{21TA}}{S_{21AM}}(1 - S_{11AM}S_{11TA}), \tag{14}$$

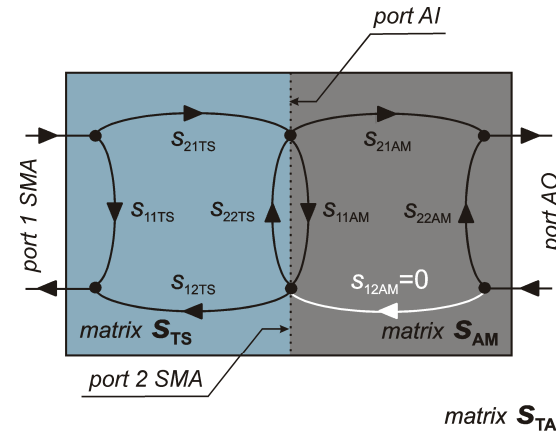where S_{AM} is the scattering matrix of the amplifier.

Figure 4. Signal flow graph of the whole system.

High standard *SE* measurements impose numerous quality requirements on the experimental setup. Since the entire signal path must be electromagnetically tight, precision coaxial connectors, semi-rigid cables, precise waveguide–coaxial transitions, precise waveguide sections, and fabric fixture are required. For waveguides, the most important elements are the quality of the flange surface and tight flange–waveguide and flange–flange connections.

4. Results and Discussion

4.1. Sample Conductivity

The sheet resistances of most samples under investigation are depicted in Figure 5. The samples not shown there had a sheet resistance that was too high to be measured, i.e., higher than 1 kΩ, which is the upper limit of the measurement instrument used in this study. The lowest sheet resistance values were reached by silver- and copper-coated woven fabrics (Figure 5a), followed by the crocheted fabric with conductive yarn. This finding can easily be explained by silver and copper having very high conductivities, with silver being the most conductive metal and copper having only around 7% lower conductivity.

Here, the more important parameters are apparently the cover factor of the metallization on the woven fabrics (i.e., the ratio of the coated area relative to the overall fabric area), which seems to be similar according to Table 1, and the conductive layer thickness, which is not given by the fabric producers. The crocheted fabric with conductive yarn contains large pores (cf. Table 1), resulting in a slightly higher sheet resistance than both metallized woven fabrics.
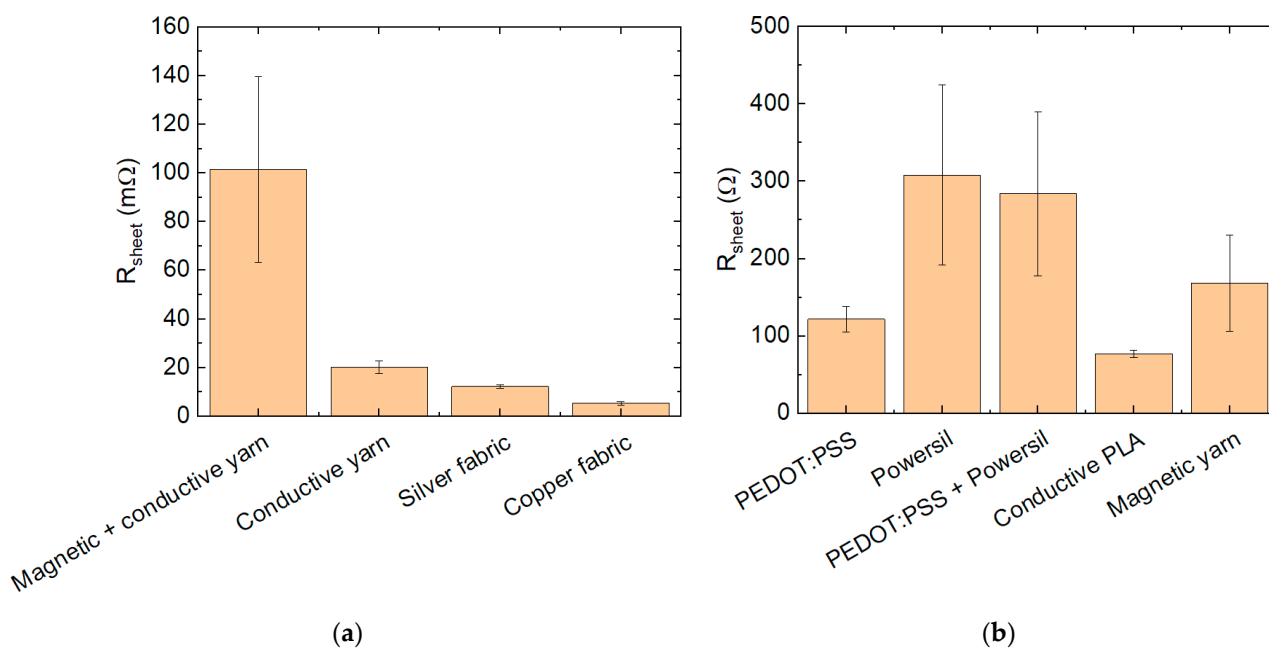

(a)   (b)

Figure 5. Sheet resistances of conductive samples: (**a**) samples with sheet resistances in the mΩ range; (**b**) samples with sheet resistances in the Ω range.

The crocheted fabric with magnetic and conductive yarn shows not only a much higher sheet resistance, but also a significantly higher standard deviation (cf. error bars in Figure 5a), which can be attributed to the large open pores and the addition of non-conductive PES yarn making it difficult to reach a proper contact between the electrode pins and the conductive part of the fabric.

Among the less conductive materials whose sheet resistances could be measured (Figure 5b), the PEDOT:PSS coating and the conductive PLA had resistances of around 100 Ω with relatively small standard deviations, while both Powersil-coated fabrics had larger and stronger varying sheet resistance. This can be explained by the hand-coating process, which leads to thickness variations of the highly viscous coating material, which is thus hard to process with constant thickness. On the other hand, the crocheted fabric from magnetic yarn contains 80% non-conductive fibers, making contacting of the conductive parts complicated.

The samples that could not be measured are pure and magnetic PLA, both of which are non-conductive, as well as both nanofiber mats that contain nanoparticles of the semi-conductor nickel ferrite and thus cannot be expected to show a high conductivity either. Moreover, the nanoparticles are embedded inside the nanofiber mat as in a non-conductive matrix and normally do not form percolation paths, so no measurable sheet resistance could be expected, even if the nanoparticles were highly conductive. Instead, these nanofiber mats belong to the magnetic samples tested here in addition to the conductive ones due to their potential to shield static magnetic fields.

These measurements suggest that silver- and copper-coated fabrics, as well as both crocheted fabrics with conductive yarn (with or without additional magnetic yarn), may have good EMI shielding effectiveness. The latter, however, have large pores that can be expected to reduce the *SE* values. Section 4.3 reports the respective measurements of the

EMI shielding effectiveness of these samples compared to the crocheted fabric with purely magnetic yarn.

4.2. Validation of the Shielding Effectiveness Measurements

The test set for shielding effectiveness measurements was validated before measuring the aforementioned samples. For this purpose, food-grade aluminum foil with a thickness of $t = 8.7$ µm was measured in the setup described above. The conductivity of the foil measured for DC with a four-point probe was 27.7 MS/m, which is lower than the conductivity of pure aluminum (35.4 MS/m). The theoretical value of the *SE* for the tested foil at 9 GHz is about 140–150 dB. Therefore, the *SE* measurement of such a material is particularly difficult due to the need to obtain a high EM tightness of the waveguide path and ensure a low noise factor of the meter.

The results of measurements and calculations of S_{21} are shown in Figure 6. As can be seen, for frequencies higher than 7 GHz, the measured values are within the limits theoretically determined for conductivities of 35.4 MS/m and 27.7 MS/m, respectively. The ripples observed in the measurements are present due to the imperfections in the SMA/WR-90 transitions (T). The increase in attenuation observed for frequencies lower than 7 GHz is due to the proximity of the TE_{10} mode cutoff frequency of 6.57 GHz. The very good agreement between the calculations and measurements obtained for the aluminum foil confirms the accuracy of the measurements in our experimental setup. Moreover, the materials considered here have relatively smaller values of *SE*, which makes their measurement easier.
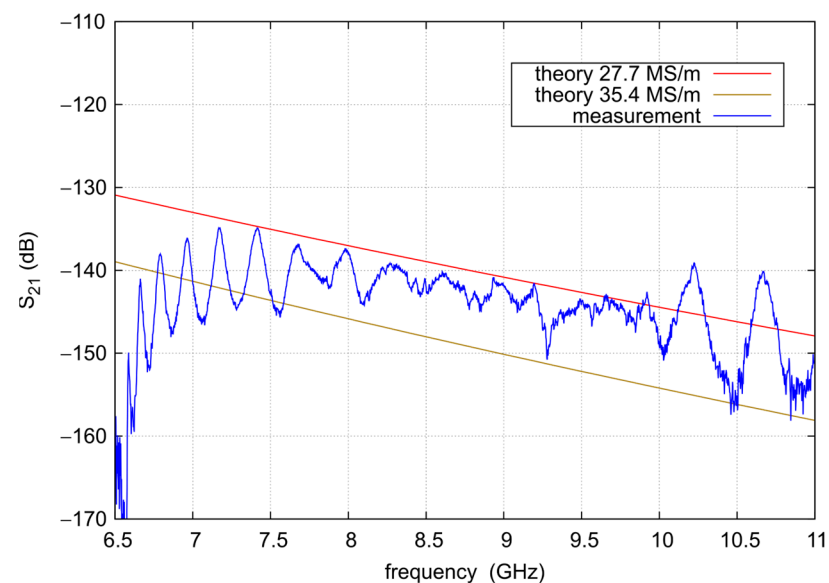

Figure 6. Results of measurements and calculations of the S_{21} coefficient for the food-grade aluminum foil.

4.3. The SE of Textile and 3D-Printed Fabrics

The textile fabrics and 3D-printed samples were tested according to the following schedule:

1. The fabric samples were mounted on the fixture within the test setup.
2. The elements of the $\mathbf{S}_{TA}$ matrix were measured.
3. The elements of the $\mathbf{S}_{TS}$ scattering matrix were determined by using the aforementioned Formulas (13) and (14).
4. The results were corrected based on the measurements of the theoretical *SE* for aluminum foil according to the formula

$$S_{21} = S_{21TS} - S_{21fm} + S_{21ft}, \tag{15}$$

where s_{21fm} is the measured transmission coefficient of the aluminum foil and S_{21ft} is the theoretical value of the transmission coefficient of the aluminum foil. The applied correction was used to minimize the influence of the test setup imperfections so that the corrected results for the aluminum foil agree with the theoretical calculations.

5. The *SE* is evaluated by means of the Formulas (6)–(8).

Figures 7 and 8 show the frequency behavior of the S_{21TS} coefficient and *SE* of the materials under examination. As expected, according to the measurements of the sheet resistance values, only five samples (silver fabric, copper fabric, conductive yarn, magnetic yarn, magnetic+conductive yarn) among the materials tested in this study showed usable *SE* values. For the others, *SE* was approximately 0 dB in the examined frequency band. It should be mentioned that the magnetic yarn samples actually have too high a sheet resistance to be expected to be suitable for EMI shielding; a potential reason for this finding is discussed below. Generally, due to the applied corrections, the influence of the test setup was significantly reduced.
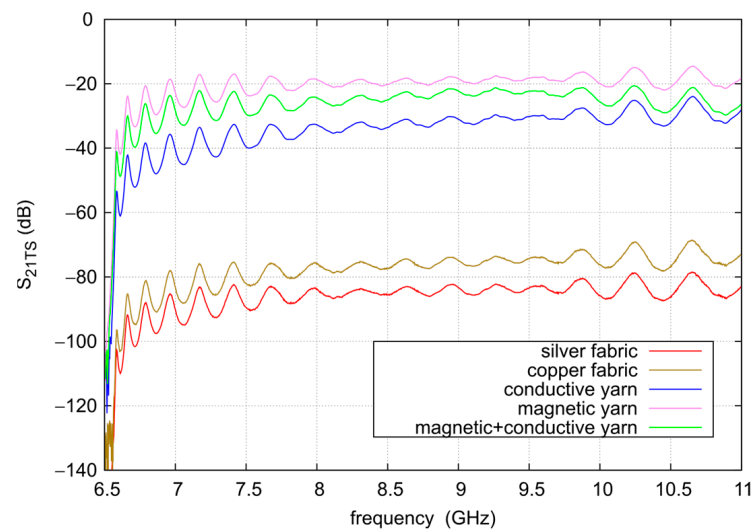

Figure 7. The S_{21TS} measurement results of the examined conductive materials versus frequency.
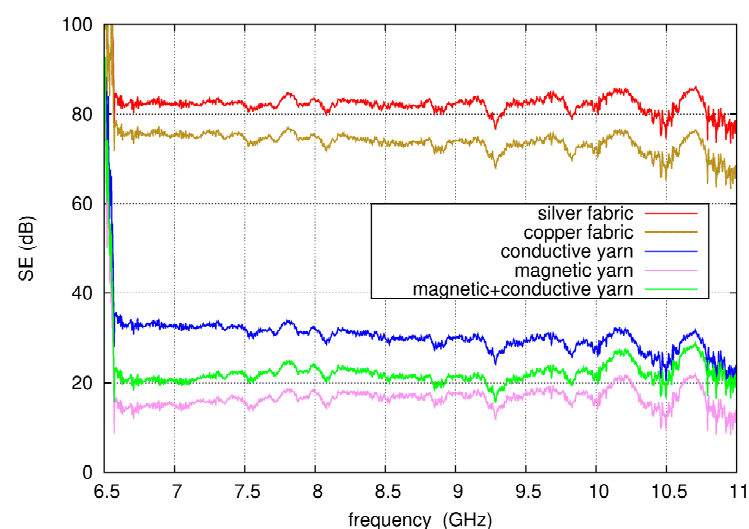

Figure 8. Evaluated *SE* of the materials examined versus frequency.

The S_{21TS} coefficients (Figure 7) show a similar frequency dependence to the S_{21} values of the aluminum foil used for calibration (Figure 6). Here, again, the ripples due to the imperfections in the SMA/WR-90 transitions can be observed as well as the increase in

attenuation for frequencies below approximately 7 GHz. More importantly, the highest attenuation along the whole investigated frequency band was found for the silver-coated fabric, directly followed by the copper-coated fabric, as would be expected from the sheet resistance measurements (Figure 5).

Interestingly, the crocheted fabrics from the conductive yarn, the magnetic+conductive yarns, and the magnetic yarn all show relatively similar values, while their sheet resistances varied by four orders of magnitude (cf. Figure 5). This can be explained by the structure of the magnetic yarns, which contain 20% conductive stainless steel fibers. These fibers are short (in the range of 10–20 mm) and thus do not often come into contact with neighboring conductive fibers in the PES fiber-based yarns, leading to a relatively low conductance for the whole yarn or crocheted fabric. At smaller scales, however, each single steel fiber has a conductance comparable to that of the silver coating on the conductive yarn. While the conductivity of silver is significantly higher than that of steel, the conductance is also influenced by an object's geometry, and the silver coatings on the fibers are in the range of 10–100 nanometers, while the steel fiber showed a thickness of 12–13 µm.

On the other hand, the textile fabrics with PEDOT:PSS coating and the 3D-printed conductive PLA sample both having lower sheet resistances than the magnetic stainless steel yarn did not show noteworthy EMI shielding, indicating that the conductive properties are not the only relevant parameter for EMI shielding effectiveness, as already discussed in several previous studies [12]. Instead, the macroscopic and microscopic sample structure also plays an important role. This finding indicates that crocheted or three-dimensional textile fabrics, e.g., knitted fabrics, should be investigated further, ideally combining their relatively thick 3D structure with significantly reduced pore sizes.

The results obtained from *SE* measurements (Figure 8) again show that there are two types of materials that have significantly different properties. The first set of samples includes the highly conductive silver and copper coatings on dense woven fabrics, for which the *SE* is about 82 dB and 74 dB, respectively. The second type is the open-pore, less conductive crocheted fabrics whose *SE* does not exceed 35 dB, but which still have a much higher EMI shielding effectiveness than the other—partly more conductive—samples under examination.

Theoretically, the *SE* should increase with frequency. According to our measurements on textile fabrics, this value is almost constant (silver and copper coating on woven fabrics) or even decreases (magnetic yarn, magnetic+conductive yarn). Only for the conductive yarn, the *SE* increases slightly with frequency. The observed differences from the theory stem from the inhomogeneous nature of the woven materials and the electrical dimensions of their pores (physical dimensions related to the operating wavelength λ), which increase with frequency. For this reason, the *SE* of the fabric can decrease with frequency.

The metalized woven fabrics show a high *SE* of around 80 dB, comparable to the value of 85 dB previously reported by another research group for a 4.5 mm thick carbon/polyamide 6 nonwoven sample [30]. Only for PPy-modified Mxene sheets coated on PET fabrics, a higher EMI shielding effectiveness of approximately 90 dB was found in a previous study [14], thus applying a much more complicated method to reach a high conductivity, as compared to using simple metallized, commercially available woven fabrics. The other *SE* values presented in the literature are significantly smaller, such as MXene-coated fabrics [31,32], different copper- or nickel-coated fabrics [33,34], carbon nanotube/graphene coatings [35], or coatings with conductive polymers [36,37]. Thus, our investigations show the great potential of some readily available metalized fabrics for shielding purposes. The future experiments will aim to improve the washability of the examined textile fabrics to increase their longevity.

5. Conclusions and Outlook

In a recent project, the *SE* values of various conductive and magnetic textile fabrics, together with some 3D-printed materials, were investigated. The fabrics crocheted from highly conductive yarns showed only low EMI shielding properties due to their large pores.

In contrast, the metalized fine woven fabrics revealed high shielding values around 80 dB, which is higher than most other textile materials with conductive coatings reported in the literature. Generally, this study shows the importance of combining small pore sizes with high conductivity, which is optimal for the metalized woven fabrics used here.

It must be mentioned that these metalized fabrics are known to be damaged by washing and sweat since the metal coating will be oxidized or even abraded under harsh conditions. The next steps will thus aim at increasing the washability and sweat resistance of the described fabrics by using conductive and nonconductive coatings while maintaining their drapability and at testing fine-knit fabrics from conductive yarns, which typically have a higher drapability and elasticity than woven fabrics. Such fabrics would often be favorable, e.g., for garments for people working in EMI-prone areas or in several technical applications, such as covering bent parts of cars or planes or flexible EMI shielding covers for laboratory instruments and machine parts. Moreover, combining the relatively thick, three-dimensional structure of crocheted or knitted fabrics with thin woven fabrics with very small pores is another promising approach to preparing new textile structures for EMI shielding with flexible, drapable fabrics.

References

1. Wang, H.; Li, S.N.; Liu, M.Y.; Zhou, Y. Review on Shielding Mechanism and Structural Design of Electromagnetic Interference Shielding Composites. *Macromol. Mater. Eng.* **2021**, *306*, 2100032. [CrossRef]
2. Peng, M.Y.; Qin, F.X. Clarification of basic concepts for electromagnetic interference shielding effectiveness. *J. Appl. Phys.* **2021**, *130*, 225108. [CrossRef]
3. Duan, Y.P.; Liu, S.H.; Guan, H.T. Investigation of electrical conductivity and electromagnetic shielding effectiveness of polyaniline composite. *Sci. Technol. Adv. Mater.* **2005**, *6*, 513–518.
4. Guan, H.T.; Chung, D.D.L. Absorption-dominant radio-wave attenuation loss of metals and graphite. *J. Mater. Sci.* **2021**, *56*, 8037–8047. [CrossRef]
5. Dai, M.W.; Zhai, Y.H.; Zhang, Y. A green approach to preparing hydrophobic, electrically conductive textiles based on waterborne polyurethane for electromagnetic interference shielding with low reflectivity. *Chem. Eng. J.* **2021**, *421*, 127749. [CrossRef]
6. Wu, J.H.; Chung, D.D.L. Increasing the electromagnetic interference shielding effectiveness of carbon fiber polymer–matrix composite by using activated carbon fibers. *Carbon* **2002**, *40*, 445–467. [CrossRef]
7. Roh, J.-S.; Chi, Y.-S.; Kang, T.J. Electromagnetic shielding effectiveness of multifunctional metal composite fabrics. *Text. Res. J.* **2008**, *78*, 825–835. [CrossRef]
8. Mocha, J.; Wójcik, D.; Surma, M. Immunity of medical electrical equipment to radiated RF disturbances. *Proc. SPIE* **2018**, *10715*, 1071507.
9. Ren, S.; Guo, S.; Liu, X.; Liu, Q. Shielding effectiveness of double-layer magnetic shield of current comparator under radial disturbing magnetic field. *IEEE Trans. Magn.* **2016**, *52*, 9401907. [CrossRef]
10. Wang, Y.; Wang, W.; Qi, Q.B.; Xu, N.; Yu, D. Layer-by-layer assembly of PDMS-coated nickel ferrite/multiwalled carbon nanotubes/cotton fabrics for robust and durable electromagnetic interference shielding. *Cellulose* **2020**, *27*, 2829–2845. [CrossRef]

11. Ghosh, S.; Remanan, S.; Mondal, S.; Ganguly, S.; Das, P.; Singha, N.; Das, N.C. An approach to prepare mechanically robust full IPN strengthened conductive cotton fabric for high strain tolerant electromagnetic interference shielding. *Chem. Eng. J.* **2018**, *344*, 138–154. [CrossRef]

12. Blachowicz, T.; Hütten, A.; Ehrmann, A. Electromagnetic Interference Shielding with Electrospun Nanofiber Mats—A Review of Production, Physical Properties and Performance. *Fibers* **2022**, *10*, 47. [CrossRef]

13. Blachowicz, T.; Wojcik, D.; Surma, M.; Magnuski, M.; Ehrmann, G.; Ehrmann, A. Textile fabrics as electromagnetic shielding materials—A review of preparation and performance. *Fibers* **2023**, *11*, 29. [CrossRef]

14. Wang, Q.-W.; Zhang, H.-B.; Liu, J.; Zhao, S.; Xie, X.; Liu, L.X.; Yang, R.; Koratkar, N.; Yu, Z.-Z. Multifunctional and Water-Resistant MXene-Decorated Polyester Textiles with Outstanding Electromagnetic Interference Shielding and Joule Heating Performances. *Adv. Funct. Mater.* **2019**, *29*, 1806819. [CrossRef]

15. Uzun, S.; Han, M.K.; Strobel, C.J.; Hantanasirisakul, K.; Goad, A.; Dion, G.; Gogotsi, Y. Highly conductive and scalable $Ti_3C_2T_x$-coated fabrics for efficient electromagnetic interference shielding. *Carbon* **2021**, *174*, 382–389. [CrossRef]

16. Yu, Z.C.; Deng, C.; Seidi, F.; Yong, Q.; Lou, Z.C.; Meng, L.C.; Liu, J.W.; Huang, C.; Liu, Y.Q.; Wu, W.B.; et al. Air-permeable and flexible multifunctional cellulose-based textiles for bio-protection, thermal heating conversion, and electromagnetic interference shielding. *J. Mater. Chem. A* **2022**, *10*, 17452–17463. [CrossRef]

17. Periyasamy, A.P.; Yang, K.; Xiong, X.M.; Venkataraman, M.; Militky, J.; Mishra, R.; Kremenakova, D. Effect of silanization on copper coated milife fabric with improved EMI shielding effectiveness. *Mater. Chem. Phys.* **2020**, *239*, 122008. [CrossRef]

18. Hu, S.; Wang, D.; Kyosev, Y.; Kremenakova, D.; Militky, J. The novel approach of EMI shielding simulation for metal coated nonwoven textiles with optimized textile module. *Polym. Test.* **2022**, *114*, 107706. [CrossRef]

19. Hong, S.W.; Yoo, S.S.; Lee, J.Y.; Yoo, P.J. Sonochemically activated synthesis of gradationally complexed Ag/TEMPO-oxidized cellulose for multifunctional textiles with high electrical conductivity, super-hydrophobicity, and efficient EMI shielding. *J. Mater. Chem. C* **2020**, *8*, 13990–13998. [CrossRef]

20. Vahle, D.; Böttjer, R.; Heyden, K.; Ehrmann, A. Conductive polyacrylonitrile/graphite textile coatings. *AIMS Mater. Sci.* **2018**, *5*, 551–558. [CrossRef]

21. Moonlek, B.; Wimolmala, E.; Markpin, T.; Sombatsompop, N.; Saenboonruang, K. Enhancing electromagnetic interference shielding effectiveness for radiation vulcanized natural rubber latex composites containing multiwalled carbon nanotubes and silk textile. *Polym. Compos.* **2020**, *41*, 396–4009. [CrossRef]

22. Zhou, L.H.; Lan, C.T.; Yang, L.; Xu, Z.Z.; Chu, C.L.; Liu, Y.C.; Qiu, Y.P. The optimization of nanocomposite coating with polyaniline coated carbon nanotubes on fabrics for exceptional electromagnetic interference shielding. *Diam. Relat. Mater.* **2020**, *104*, 107757. [CrossRef]

23. Abdelal, N. Electromagnetic interference shielding of stitched carbon fiber composites. *J. Ind. Text.* **2020**, *49*, 773–790. [CrossRef]

24. Pakdel, E.; Kashi, S.; Baum, T.; Usman, K.A.S.; Razal, J.M.; Varley, R.; Wang, X.G. Carbon fibre waste recycling into hybrid nonwovens for electromagnetic interference shielding and sound absorption. *J. Clean. Prod.* **2021**, *315*, 128196. [CrossRef]

25. Hu, Q.L.; Duan, Y.F.; Zheng, X.H.; Nie, W.Q.; Zou, L.H.; Xu, Z.Z. Lightweight, flexible, and highly conductive recycled carbon fiber felt for electromagnetic interference shielding. *J. Alloys Comp.* **2023**, *935*, 168152. [CrossRef]

26. Rybicki, T.; Stempien, Z.; Karbownik, I. EMI Shielding and Absorption of Electroconductive Textiles with PANI and PPy Conductive Polymers and Numerical Model Approach. *Energies* **2021**, *14*, 7746. [CrossRef]

27. Siavashani, V.S.; Gursoy, N.C.; Montazer, M.; Altay, P. Stretchable Electromagnetic Interference Shielding Textile Using Conductive Polymers and Metal Nanoparticles. *Fibers Polym.* **2022**, *23*, 2748–2759. [CrossRef]

28. Yu, Z.C.; Zhao, Y.H.; Liu, J.R.; Wang, Y.S.; Qin, Y.; Zhu, Z.Y.; Wu, C.; Peng, J.C.; He, H.L. Advancement in cellulose-based multifunctional high conductive PNIPAAm/PPy hydrogel/cotton composites for EMI shielding. *Cellulose* **2022**, *29*, 6963–6981. [CrossRef]

29. Schelkunoff, S.A. *Electromagnetic Waves*; Van Nostrand Company: New York, NY, USA, 1945.

30. Pozar, D.M. *Microwave Engineering*, 3rd ed.; John Wiley & Sons: Hoboken, NJ, USA, 2005.

31. Pocai, M.; Dotto, I.; Festa, D. Three methods for measuring the Shielding Effectiveness of shielding materials: A comparison. In Proceedings of the 2012 IEEE International Symposium on Electromagnetic Compatibility, Pittsburgh, PA, USA, 6–10 August 2012; pp. 663–668.

32. Costa, F.; Borgese, M.; Degiorgi, M.; Monorchio, A. Electromagnetic Characterisation of Materials by Using Transmission/Reflection (T/R) Devices. *Electronics* **2017**, *6*, 95. [CrossRef]

33. Lin, H.N.; Chen, Y.Y.; Tsai, H.Y.; Lin, M.S. Characteristic Analysis and Applications of Electromagnetic Shielding Materials for Wireless Communications Device. *Open Mater. Sci. J.* **2016**, *10*, 44–53. [CrossRef]

34. Morari, C.; Balan, I. Methods for determining shielding effectiveness of materials: EEA. *Electroteh. Electron. Autom.* **2015**, *63*, 126–136.

35. Zheng, X.H.; Wang, P.; Zhang, X.S.; Hu, Q.L.; Wang, Z.Q.; Nie, W.Q.; Zou, L.H.; Li, C.L.; Han, X. Breathable, durable and bark-shaped MXene/textiles for high-performance wearable pressure sensors, EMI shielding and heat physiotherapy. *Compos. A Appl. Sci. Manuf.* **2022**, *152*, 106700. [CrossRef]

36.   Hu, S.; Wang, D.; Periyasamy, A.P.; Kremenakova, D.; Militky, J.; Tunak, M. Ultrathin Multilayer Textile Structure with Enhanced EMI Shielding and Air-Permeable Properties. *Polymers* **2021**, *13*, 4176. [CrossRef] [PubMed]
37.   Moazzenchi, B.; Montazer, M. Click electroless plating of nickel nanoparticles on polyester fabric: Electrical conductivity, magnetic and EMI shielding properties. *Colloids Surf. A Physicochem. Eng. Asp.* **2019**, *571*, 110–124. [CrossRef]